Journal for
ImmunoTherapy of Cancer

Bispecific antibodies targeting CD40 and tumor-associated antigens promote cross-priming of T cells resulting in an antitumor response superior to monospecific antibodies

Karin Hägerbrand,[1] Laura Varas,[1] Adnan Deronic,[1] Barnabas Nyesiga,[1] Anette Sundstedt,[1] Lill Ljung,[1] Christina Sakellariou,[2] Doreen Werchau,[1] Mia Thagesson,[1] David Gomez Jimenez [ORCID],[2] Lennart Greiff,[3] Mona Celander,[1] Kristine Smedenfors,[1] Anna Rosén,[1] Deniz Bölükbas,[1] Fredrika Carlsson,[1] Mattias Levin,[1] Anna Säll,[1] Laura von Schantz,[1] Malin Lindstedt,[1,2] Peter Ellmark [ORCID] [1,2]

[1]Alligator Bioscience AB, Medicon Village, Lund, Sweden
[2]Department of Immunotechnology, Lund University, Lund, Sweden
[3]Department of ORL, Head & Neck Surgery, Skåne University Hospital, Lund, Sweden

Correspondence to
Dr Peter Ellmark;
pek@alligatorbioscience.com

ABSTRACT

Background Indications with poor T-cell infiltration or deficiencies in T-cell priming and associated unresponsiveness to established immunotherapies represent an unmet medical need in oncology. CD40-targeting therapies designed to enhance antigen presentation, generate new tumor-specific T cells, and activate tumor-infiltrating myeloid cells to remodel the tumor microenvironment, represent a promising opportunity to meet this need. In this study, we present the first in vivo data supporting a role for tumor-associated antigen (TAA)-mediated uptake and cross-presentation of tumor antigens to enhance tumor-specific T-cell priming using CD40×TAA bispecific antibodies, a concept we named Neo-X-Prime.

Methods Bispecific antibodies targeting CD40 and either of two cell-surface expressed TAA, carcinoembryonic antigen-related cell adhesion molecule 5 (CEA) or epithelial cell adhesion molecule (EpCAM), were developed in a tetravalent format. TAA-conditional CD40 agonism, activation of tumor-infiltrating immune cells, antitumor efficacy and the role of delivery of tumor-derived material such as extracellular vesicles, tumor debris and exosomes by the CD40×TAA bispecific antibodies were demonstrated in vitro using primary human and murine cells and in vivo using human CD40 transgenic mice with different tumor models.

Results The results showed that the CD40×TAA bispecific antibodies induced TAA-conditional CD40 activation both in vitro and in vivo. Further, it was demonstrated in vitro that they induced clustering of tumor debris and CD40-expressing cells in a dose-dependent manner and superior T-cell priming when added to dendritic cells (DC), ovalbumin (OVA)-specific T cells and OVA-containing tumor debris or exosomes. The antitumor activity of the Neo-X-Prime bispecific antibodies was demonstrated to be significantly superior to the monospecific CD40 antibody,

WHAT IS ALREADY KNOWN ON THIS TOPIC

⇒ Bispecific CD40 antibodies have emerged as a new approach to target CD40 in a more efficient and safe manner compared with monospecific therapies. We and others have suggested that bispecific antibodies targeting CD40 and tumor-associated antigens (TAA) can enhance priming of tumor-specific T cells by both tumor-localized CD40 activation and by enhancing tumor neoantigen delivery to dendritic cells via tumor debris, extracellular vesicles and exosomes.

WHAT THIS STUDY ADDS

⇒ In this study we demonstrate that CD40×TAA bispecific antibodies can induce enhanced T-cell cross-priming superior to monospecific CD40 antibodies using in vivo models. Further, we demonstrate that this concept, using bispecific antibodies targeting both epithelial cell adhesion molecule (EpCAM) and carcinoembryonic antigen (CEA), translates into superior antitumor effects compared with monospecific CD40 antibodies, and induces T-cell dependent antitumor memory.

HOW THIS STUDY MIGHT AFFECT RESEARCH, PRACTICE OR POLICY

⇒ The mechanism described in this study demonstrates that CD40×TAA bispecific antibodies provide a new opportunity to enhance cross-priming of T cells. This class of TAA-conditional CD40 agonists has the potential to meet key needs in immuno-oncology by increasing the quantity and quality of tumor-specific T cells and at the same time remodel the tumor microenvironment through myeloid cell activation, making the tumor more inflamed.

and the resulting T-cell dependent antitumor immunity was directed to tumor antigens other than the TAA used for targeting (EpCAM).

Conclusions The data presented herein support the hypothesis that CD40×TAA bispecific antibodies can engage tumor-derived vesicles containing tumor neoantigens to myeloid cells such as DCs resulting in an improved DC-mediated cross-priming of tumor-specific CD8+ T cells. Thus, this principle may offer therapeutics strategies to enhance tumor-specific T-cell immunity and associated clinical benefit in indications characterized by poor T-cell infiltration or deficiencies in T-cell priming.

BACKGROUND

Therapy with immune checkpoint inhibitors (ICI) has revolutionized the treatment of cancer and provides a potential cure for patients with advanced metastatic cancer. However, responses to ICI therapy depend on a pre-existing immune response in the tumor microenvironment (TME) with infiltrating CD8+ T cells, and tumors with poor T-cell infiltration or deficiencies in T-cell priming still represent an unmet medical need.[1] One promising approach to overcome resistance to ICI is CD40-targeting therapies designed to enhance antigen presentation, generate new tumor-specific T cells, and activate tumor-infiltrating myeloid cells to remodel the TME.[2] CD40-targeting therapies developed specifically to increase priming of tumor-specific T cells would thus have the potential to both increase response rates in indications where programmed death ligand-1 therapies currently are approved but have limited activity, and to expand the number of indications eligible for immunotherapies.

CD40 is a member of the tumor necrosis factor receptor superfamily expressed on the surface of immune cells such as dendritic cells (DCs), B cells and macrophages, but also on other cells including epithelial, endothelial, and neoplastic cells.[3 4] DCs are highly specialized antigen-presenting cells (APCs) that are essential in the initiation of cytotoxic T lymphocyte (CTL) responses against cancers.[5 6] Signaling through CD40 promotes the ability of DCs to prime T-cell responses by inducing upregulation of the antigen presentation machinery, costimulatory molecules including CD80 and CD86, and promoting the production of cytokines including interleukin (IL)-12.[7–9] Indeed, CD40 signaling on DCs can be sufficient for the induction of an efficient CTL response.[10] Further, in studies where different DC targets are compared for their ability to induce T-cell cross-priming following treatment with antigen-conjugated antibodies, CD40 stands out as the most effective DC target compared with, for example, DEC-205 and Dectin-1 in terms of CD8+ T-cell priming.[11] Moreover, preclinical studies with CD40-targeting antibodies have shown promising antitumor effects that are dependent on the presence of T cells and DCs.[12–15] While CD40 signaling in DCs has the potential to increase the tumor-targeting T-cell pool, CD40 signaling in macrophages could additionally promote a less immunosuppressive TME.[4]

Evidence of clinical benefit of immunotherapy with agonistic CD40 antibodies as single agents or in combination with chemotherapy or ICI are emerging[16 17] and several second generation CD40 agonists are in clinical development.[16] Development of third generation CD40 targeting therapies either as bispecific antibodies (bsAbs) or fusion proteins is currently underway.[18 19] A novel approach called Neo-X-Prime has been developed by us and aims to increase the efficacy of CD40-targeting therapies.[20] This approach is based on bsAbs targeting highly expressed tumor-associated antigens (TAA, herein it refers to TAA overexpressed on the surface of tumor cells) and a cross-linking-dependent CD40 antibody. The resulting CD40×TAA bsAbs are designed to induce CD40-agonistic activity and direct tumor-derived vesicles (tumor debris, extracellular vesicles (EV) and exosomes) to APCs in the TME, which would facilitate efficient uptake and cross-presentation of neoantigens contained within the tumor vesicles. Through its superior ability to promote CD8+ T-cell priming, CD40 is a uniquely well-suited target for this approach compared with other receptors expressed by DCs.[11 21 22]

In this study, the Neo-X-Prime concept is demonstrated using CD40×TAA bsAbs generated in the RUBY format targeting two different TAA, epithelial cell adhesion molecule (EpCAM) and carcinoembryonic antigen-related cell adhesion molecule 5 (CEACAM5 or CEA), respectively. We show that the CD40×TAA bsAbs, but not the CD40 monoclonal antibody (mAb), have the capacity to cluster tumor-derived cellular debris with CD40-expressing APCs. Further, we demonstrate improved cross-priming of tumor-targeting T cells, and significantly stronger antitumor effects by administration of the bsAbs as compared with the CD40 mAb.

METHODS

Antibodies and reagents

The CD40-targeting and human CEA-targeting antibody binders, and the isotype control, were isolated from Alligator's proprietary antibody libraries. The bsAbs CD40×EpCAM and CD40×CEA and the bsAb isotype controls GFP×EpCAM and GFP×CD40 were generated in the bispecific tetravalent RUBY format (figure 1A, see also online supplemental figure S1). The CD40 mAb contains the same antibody fragment as CD40×EpCAM. The isotype×EpCAM control bsAb was generated using the same EpCAM-specific antibody fragment as the CD40×EpCAM bsAb. The isotype×CD40 bsAb was generated using the same CD40-specific antibody fragment as the CD40×CEA bsAb. The Fc domain used for all bsAbs was IgG1 containing LALA double mutations to reduce FcγR affinities.[23] The Fc-domain of the anti-CD40 mAb was wild type (wt) IgG1. The FcγR cross-linking independent (superagonist) CD40 antibody (21.4.1) was generated with IgG2 Fc.

A list of antibodies used for flow cytometry is provided in online supplemental table 1. H-2Kb/SIINFEKL MHC I tetramer-APC (Tetramer Shop) was used to stain ovalbumin (OVA)-specific T cells. CellTrace Violet (Molecular Probes) was used for analysis of proliferating T cells.
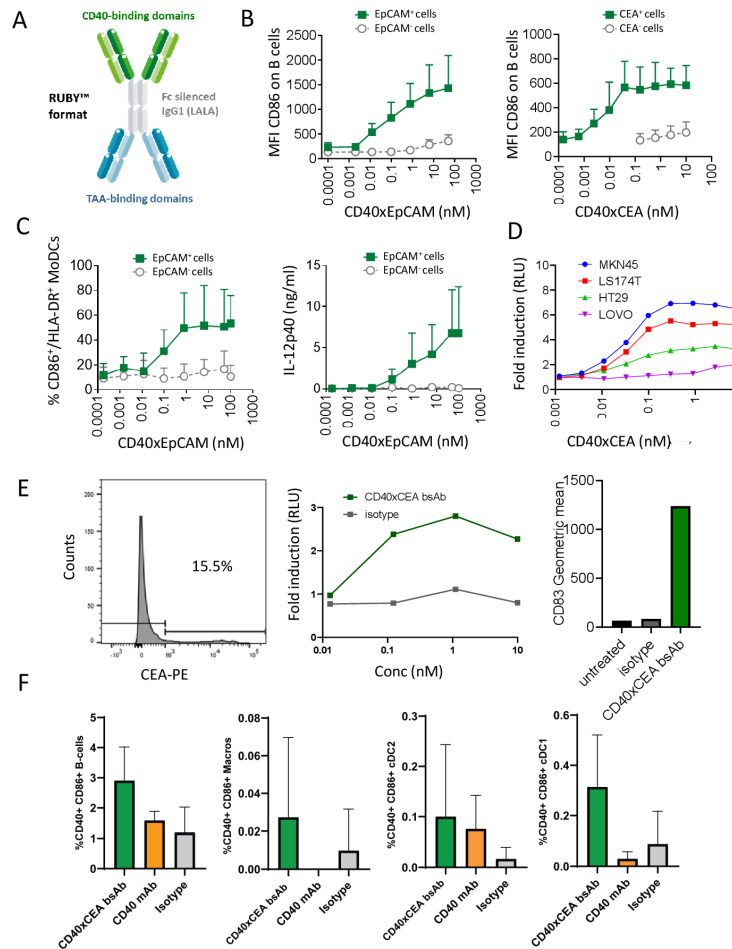
Figure 1 Simultaneous binding of CD40 and TAA by CD40×TAA bsAbs mediates activation of APCs. (A) Schematic illustration of CD40×TAA bsAbs in the RUBY format. (B) Human primary B cells were co-cultured with UV-irradiated CHO cells transfected with human EpCAM, human CEA or an empty vector in the presence of bsAbs CD40×EpCAM or CD40×CEA. After 48 hours culture, cells were harvested and the expression of CD86 on the surface of CD19+ B cells was analyzed by flow cytometry. The graphs show pooled results (mean+SD) of three donors in one representative experiment of three (EpCAM) or pooled results from five donors (CEA). (C) Human MoDCs were co-cultured with UV-irradiated CHO cells transfected with human EpCAM or an empty vector in the presence of GM-CSF, IL-4 and bsAb CD40×EpCAM. After 48 hours culture, supernatants and cells were harvested. The frequencies of activated CD14− CD1a+ DCs, double positive for CD86 and HLA-DR, were assessed by flow cytometry, and the IL-12p40 content in the supernatant was analyzed by ELISA. The graphs show pooled results (mean+SD) of six donors from four experiments. (D) CD40 activation measured in a CD40 reporter cell assay co-cultured with human cell lines expressing different levels of CEA. (E) Dissociated cells from human colorectal cancer tumors were analyzed for: (left) their CEA-expression (gated on total viable cells), (middle) ability to provide cross-linking to CD40×CEA Neo-X-Prime bsAb in a CD40 reporter assay, and (right) CD83 upregulation following stimulation of the tumor infiltrating immune cells (gated on viable CD45+CD3–CD56– cells) using CD40×CEA Neo-X-Prime bsAb or isotype×CD40 bsAb (data from one representative experiment out of three). (F) Simultaneous binding of CD40 and CEA by CD40×CEA bsAbs mediates activation of tonsillar cancer APCs in vitro. Human CD45+ HLA-DR+ CD3– cells from a tonsillar cancer biopsy were co-cultured with UV-irradiated CHO cells transfected with human CEA in the presence of CD40×CEA bsAb, CD40 mAb or isotype×CD40 bsAb. After 13 hours culture, cells were harvested and the frequencies of CD86+ CD40+ cells were investigated using flow cytometry of CD19+CD20+ B cells, CD14+ macrophages, CD1c+cDC2s and XCR1+cDC1s. APC, antigen-presenting cells; bsAb, bispecific antibodies; CEA, carcinoembryonic antigen; CHO, Chinese hamster ovarian; DC, dendritic cells; EpCAM, epithelial cell adhesion molecule; IL, interleukin; mAb, monoclonal antibody; MoDC, monocyte derived DC; UV, ultraviolet; TAA, tumor-associated antigens; GM-CSF, Granulocyte-macrophage colony-stimulating factor.

Fixable viability stain 450 or Fixable viability stain 780 (BD Biosciences) were used to exclude dead cells from the analyses.

Cell lines

Chinese hamster ovarian (CHO, European Collection of Authenticated Cell Cultures (ECACC)) cells were transfected to stably express human EpCAM, CEA or transfected with an empty vector to generate control cells. CHO cells were cultured in Roswell Park Memorial Institute Medium (RPMI) 1640 supplemented with 10% fetal calf serum (FCS), 10 mM 4-(2-hydroxyethyl)-1-piperazin eethanesulfonic acid (HEPES) and 0.6 mg/mL G418 as

selection pressure for transfected cells. MB49 cells were obtained from Millipore.

MB49 bladder cancer cells were transfected to stably express human EpCAM or CEA, generating MB49-EpCAM and MB49-CEA single cell clones. The MB49-EpCAM cells were subsequently transfected to express membrane bound OVA, generating an MB49-EpCAM-OVA single cell clone. MB49-wt cells were cultured in Dulbecco's Modified Eagle Medium (DMEM) supplemented with 10% FCS. 0.25 ug/mL puromycin was added for culturing MB49-EpCAM cells, 0.25 µg/mL puromycin plus 800 µg/mL hygromycin B for MB49-EpCAM-OVA cells and 1 mg/mL G418 for MB49-CEA cells.

Raji cells (American Type Culture Collection (ATCC)) were cultured in RPMI 1640 supplemented with 1 mM HEPES and 10% FCS. JAR cells (ATCC) were cultured in RPMI 1640 supplemented with 10% FCS. MKN45 cells (Deutsche Sammlung von Mikroorganismen und Zellkulturen (DSMZ)) were cultured in RPMI 1640 supplemented with 20% FCS. LS174T (DSMZ) were cultured in RPMI 1640 supplemented with 10% FCS, HT29 (ATCC) were cultured in McCoy supplemented with 10% FCS, LOVO (DSMZ) were cultured in RPMI 1640 supplemented with 10% FCS, and B16.F10 cells (ATCC) were cultured in DMEM supplemented with 10% FCS.

B cell activation assay
B cells were isolated from human peripheral blood mononuclear cells (Laboratory Medicine, Skåne University Hospital, Lund, Sweden) by magnetic-activated cell sorting (MACS) using human B cell isolation kit II according to the manufacturer's protocol (Miltenyi Biotech). CHO-EpCAM, CHO-CEA or CHO-control cells (untransfected or transfected with an empty vector) were ultraviolet (UV) irradiated and seeded in tissue culture-treated 96-well flat-bottom plates. B cells were co-cultured with CHO cells in the presence of recombinant human IL-4 (Gibco, 10 ng/mL) and titrated concentrations of CD40×EpCAM or CD40×CEA. After 2 days, B cells were harvested and expression level of the activation marker CD86 on $CD19^+$ B cells was analyzed by flow cytometry using FACSVerse (BD Biosciences).

DC activation assay
Monocytes were isolated from human peripheral blood mononuclear cells (Laboratory Medicine) by MACS using CD14 microbeads (Miltenyi Biotech) according to the manufacturer's protocol. Human monocyte derived DCs (MoDCs) were generated by culturing monocytes for 7 days in the presence of granulocyte-macrophage colony-stimulating factor (GM-CSF, 150 ng/mL, Gibco) and IL-4 (50 ng/mL, Gibco). CHO-EpCAM or CHO-control cells were UV irradiated and seeded in tissue culture-treated 96-well flat-bottom plates. DCs were co-cultured with CHO cells in the presence of GM-CSF, IL-4 and titrated concentrations of CD40×EpCAM. After 2 days, DCs were harvested and expression of HLA-DR and CD86 on $CD14^-$ $CD1a^+$ DCs was analyzed by flow cytometry using FACSVerse. Supernatants were collected and IL-12p40 content was measured by ELISA (BioLegend).

Reporter assays
A CD40 bioassay (Promega, Wisconsin, USA) was used according to the manufacturer's protocol. Briefly, 15,000 CD40 effector cells were plated on 96-well plates (Thermo Scientific, 136101) and incubated in a 37°C, 5% CO2 incubator overnight. Next, the supernatant was aspirated, and corresponding concentrations of ATOR-4066 or controls were added into the wells. Primary human tumor-derived cells from patients with colorectal cancer (described below) or cell-lines were co-cultured with the CD40 effector cells for an additional 6 hours in a 37°C, 5% CO2 incubator. Then, the plate was taken out to room temperature to equilibrate for 10–15 min. Finally, Bio-Glo Reagent was added into each well and the luminescence signal was measured using FLUOstar Optima plate reader (BMG Labtech). The data was analyzed with GraphPad Prism V.9.4.0 software (GraphPad software) and displayed as Fold induction (RLU): RLU activated/RLU untreated.

Functional assays using cells obtained from primary human tumors
Dissociated primary tumor-derived cells (DTCs) from patients with colorectal cancer were purchased from Discovery Life Sciences (Huntsville, Alabama, USA). Directly after thawing, DTCs were counted using Nucleo-Counter NC-200 (ChemoMetec) and 200,000 viable cells were pipetted into an Nunc UpCell 96-well plate (Thermo Scientific, 174897), followed by addition of ATOR-4066 or controls. The plate was incubated for 48 hours in a 37°C, 5% CO2 incubator. Next, the cells were harvested, and analyzed by flow cytometry. For basal levels of CEA-expression, the DTCs were stained with a CD66abce antibody (online supplemental table 1) and analyzed by flow cytometry.

The tonsillar cancer biopsy was cut into small fragments in RPMI 1640 medium (Thermo Fisher Scientific) supplemented with 0.1 mg/mL gentamycin (Sigma-Aldrich). The tissue fragments were enzymatically digested with collagenase IV (2.0 mg/mL) and DNase I (Sigma-Aldrich) (200 Kunits/mL) for 20 min at 37°C. Cells were filtered using a 70 µm cell strainer and stained with CD3-PerCPCy5.5, versus 620-PECF594, CD45-APCH7 and HLA-DR-BV711 for cell sorting using FACSAria IIu (BD Biosciences). 10^4 viable $CD45^+$ $HLA-DR^+$ $CD3^-$ cells were sorted directly into 96-well flat-bottom plates (Nunc UpCell, Thermo Fisher Scientific) pre-seeded with $6×10^4$ UV-irradiated CHO-CEA cells per well. 19 nM of CD40×CEA bsAbs, CD40 mAbs or isotype controls were added to the co-cultures for 13 hours, after which the supernatants were collected, and the cells were washed and blocked for non-specific binding with ChromPure mouse IgG (Jackson ImmunoResearch) for 15 min at room temperature. Cells were immediately stained with fluorochrome-coupled antibodies (online supplemental table 1) for flow cytometric analysis using an FACSAria IIu instrument.

Tumor cell line debris clustering assay

EpCAM$^+$ JAR cells and MB49 CEA-expressing cells were labeled with the fluorescent dye PKH26 (Sigma-Aldrich) according to manufacturer's instructions. Labeled JAR cells, MB49 wt or MB49-CEA cells were heat-shocked at 45°C for 10 min to induce necrosis, followed by incubation at 37°C overnight. The heat-shocked cells were then centrifuged and the supernatant containing necrotic tumor cell line debris was collected. Raji cells were labeled with the nuclear dye Hoechst 33,342 (Thermo Scientific) and cultured with necrotic debris and titrated antibodies (CD40×EpCAM, CD40×CEA or anti-CD40 mAb). Images were captured using a Cytation 5 live cell imager (BioTek) and the number of PKH26-stained tumor debris co-localized with Hoechst-stained Raji cells was quantified using Gen5 software (BioTek).

Mice

Human CD40 transgenic mice (hCD40tg)[12] were bred and maintained at the Medicon Village animal facility (Lund, Sweden). C57BL/6 and C57BL/6-Tg(TcraTcrb)1100Mjb/J (OT-1) mice were obtained from Janvier and Charles River, respectively. Mice used for experiments were between 8 and 14 weeks of age. All experiments were performed after approval from the Malmö/Lund Animal Ethics Committee, No: 16318/2019.

Isolation of murine cells

Spleens from OT-1 mice were passed through 70 µm cell strainers (Fisherbrand) and CD8$^+$ T cells were isolated by MACS using the mouse CD8$^+$ T-cell isolation kit (Miltenyi Biotech). Isolated OT-1 T cells were labeled with Cell-Trace Violet (Molecular Probes) according to manufacturer's instructions (Invitrogen).

For isolation of DCs, spleens from hCD40tg mice were cut in small pieces and incubated at 37°C with 0.38 mg/mL Liberase TL (Roche) and 0.1 mg/mL DNase I (Roche) for 30 min. After incubation, the supernatants were collected and remaining tissue pieces were passed through a 70 µm cell strainer. DCs were isolated by MACS using CD11c microbeads (Miltenyi Biotech) according to the manufacturer's protocol.

Imaging of murine DC T-cell tumor debris co-cultures

MB49-EpCAM-OVA cells were labeled with the fluorescent dye PKH67 (Sigma-Aldrich), heat-shocked at 45°C for 10 min to induce necrosis, followed by incubation at 37°C overnight. The heat-shocked MB49-EpCAM-OVA cells were then co-cultured with hCD40tg DCs labeled with CellTracker Deep Red (Invitrogen) and CellTrace Violet-labeled OT-1 T cells. Images were captured using a Cytation 5 live cell imager.

T-cell priming assays using murine DC T-cell co-cultures

MB49-EpCAM-OVA cells were heat-shocked at 45°C for 10 min to induce necrosis, followed by incubation at 37°C overnight. Alternatively, MB49-EpCAM-OVA were cultured to 100% confluency, cell culture media was collected and exosomes were isolated using Total

Exosome Isolation kit (Invivogen). Exosomes were further purified by filtering through an Amicon Ultra-15 Centrifugal Filter (Millipore) and a 0.22 µm Millex-GV syringe filter (Millipore). The purity of exosomes was analyzed using Uncle (Unchained Labs), and exosome yield was quantified using a BCA Protein Assay (Pierce). hCD40tg DCs were co-cultured with CellTrace Violet-labeled OT-1 T cells and necrotic debris or exosomes from MB49-EpCAM-OVA cells in the presence of 5 nM or 100 nM CD40×EpCAM bsAb, respectively, or control antibodies for 72 hours. OT-1 T-cell proliferation was assessed using an FACSVerse.

In vivo models

For antitumor effect studies, solid tumors were established in hCD40tg mice by subcutaneous (s.c.) inoculation in the flank with 0.25×10^6 MB49-EpCAM or MB49-wt cells on day 0. On days 10 and 13, tumor-bearing mice were treated with intraperitoneal (i.p.) injections of vehicle (phosphate-buffered saline, PBS) or antibodies, including CD40×EpCAM bsAb, anti-CD40 mAb or isotype-EpCAM bsAb at indicated doses. Tumor volume was measured at least two to three times per week with a caliper and calculated as (width/2×length/2×height/2) ×4 p/3. Animals were sacrificed when ethical endpoints were reached (including tumor volume exceeding 2 cm^3, tumor ulceration or affected health) or at termination of the experiment. Mice that were completely cured from their tumors (complete responders, CR) were used for re-challenge studies where CR or naïve mice were inoculated with 0.25×10^6 MB49-EpCAM or MB49-wt cells, or 0.1×10^6 B16.F10 cells.

For T-cell depletion studies, CR and naïve mice were treated with PBS or a mixture of 10 mg/kg anti-CD4 mAb (clone GK1.5) and 10 mg/kg anti-CD8a mAb (clone 53-6.7; BioXCell) on days −2, −1, 0, 4, 8, 11 and 15. 0.25×10^6 MB49-EpCAM cells were inoculated s.c. on day 0.

For studying systemic immune activation, hCD40tg mice were inoculated with 0.25×10^6 MB49-EpCAM cells on day 0 followed by i.p. treatment with vehicle (PBS), CD40×EpCAM bsAb, anti-CD40 mAb or anti-CD40 super-agonist (clone 21.4.1) on days 10, 13 and 16 at indicated doses. Blood samples were collected 4 hours after treatment on day 13 and IL-6 levels were analyzed in plasma by ELISA (eBioscience). Plasma samples from day 13 were also analyzed using a 19-plex mouse cytokine MSD panel (Meso Scale Discovery). At termination on day 20, the spleens were removed and weighed.

For studies of antigen-specific T-cell responses in vivo, hCD40tg mice were inoculated with 0.25×10^6 MB49-EpCAM-OVA cells on day 0. On day 17, the mice were adoptively transferred with OT-1 T cells isolated as described above, followed by treatment with PBS, CD40×EpCAM bsAb or anti-CD40 mAb on day 18. On day 19, mice were treated with FTY720 (Cayman Chemical) i.p. to prevent egress of T cells from lymph nodes. On day 21, tumor-draining lymph nodes were collected,

passed through 70 µm cell strainers to generate single-cell suspensions, and the presence of OT-1 T cells was analyzed by flow cytometry using an FACSVerse.

Statistical analyzes

Statistical significance was evaluated using GraphPad Prism V.9.3.1 (GraphPad software).

RESULTS

Simultaneous binding of CD40 and TAA mediates TAA-dependent activation of CD40-expressing APCs

The CD40×EpCAM and CD40×CEA bsAbs were generated in the RUBY format, with LALA mutations in the Fc region to abolish FcγR mediated multimerization (figure 1A, and online supplemental figure S1), resulting in bsAbs that require binding to their respective TAA to induce multimerization and subsequent CD40 signaling. TAA-dependent cross-linking was demonstrated for both the CD40×EpCAM and CD40×CEA bsAbs as dose-dependent upregulation of CD86 on human primary B cells occurred in the presence of EpCAM⁺ and CEA⁺ cells, respectively, but not the corresponding EpCAM⁻/CEA⁻ control cells (figure 1B). The EpCAM-dependent CD40 agonistic effect of the CD40×EpCAM bsAb was further evaluated using human MoDCs. When cross-linked by EpCAM⁺ cells, but not when cultured with EpCAM⁻ control cells, CD40×EpCAM induced a dose-dependent increase in CD86 and HLA-DR double-positive DCs and a concomitant increase in the amount of IL-12p40 released into the culture supernatant (figure 1C). The ability of CD40×CEA bsAb to activate CD40-expressing reporter cells in the presence of cell lines expressing different levels of CEA was also investigated (figure 1D), demonstrating that the level of CD40 activation correlates to CEA density and that only very low levels of activity is obtained at CEA densities around 5000 CEA/cell (online supplemental table 2). Further, the CEA densities in patient derived tumor cells were sufficient to provide cross-linking and induce CD40 stimulation in the same reporter cell assay (figure 1E, middle graph), demonstrating that the cell lines and systems used are translatable to the clinical setting. Moreover, when culturing dissociated cells from patient derived colon tumors, it was demonstrated that a CD40×CEA bsAb could activate tumor infiltrating immune cells (figure 1E, right graph). This was further studied using cell-sorted APC from a patient with tonsillar cancer, suggesting that CD40×CEA bsAb stimulate activation of B cells, macrophages, cDC2s and cDC1s (figure 1F).

Neo-X-Prime CD40×TAA bsAbs mediate localization of tumor debris to APCs and promote activation of antigen-specific T cells

Expression levels of CD40, EpCAM and CEA on Raji cells, JAR cells and transfected MB49-CEA cells, respectively, were verified using flow cytometry (figure 2A). The ability of the CD40×EpCAM bsAb to facilitate delivery of tumor-derived material to CD40⁺ APCs was assessed in vitro using live imaging of fluorescently labeled CD40⁺ Raji cells cultured in the presence of necrotic debris from the EpCAM expressing JAR tumor cell line (figure 2B). The CD40×EpCAM bsAb but not the control CD40 mAb formed clusters of JAR-derived tumor cell debris with Raji cells in a dose-dependent manner (figure 2C). A similar dose-dependent clustering of necrotic debris from a CEA-transfected MB49 tumor cell line with Raji cells was seen with the CD40×CEA bsAb. The lack of clustering observed with MB49 wt-derived debris indicates that engagement of CEA is required for CD40×CEA-mediated delivery of debris to APCs (figure 2C).

To investigate cross-priming of tumor antigen-specific T cells in the presence of the CD40×EpCAM bsAb, we generated double-transfected MB49 tumor cells expressing human EpCAM and a membrane-bound form of chicken OVA. Imaging of co-cultured DCs isolated from hCD40tg mice, CD8⁺ T cells isolated from OVA-specific TCR transgenic (OT-1) mice and necrotic MB49-EpCAM-OVA cells indicated that the cells cluster together in the presence of CD40×EpCAM bsAbs (figure 2D). Flow cytometry analysis of similar co-cultures demonstrated increased proliferation of OT-1 T cells in the presence of CD40×EpCAM bsAb compared with CD40 mAb or an EpCAM monotargeting control bsAb (isotype×EpCAM) (figure 2E). Similar results were observed when hCD40tg DCs and OT-1 T cells were cultured with exosomes isolated from MB49-EpCAM-OVA cells and the CD40×EpCAM bsAb (figure 2F). These data support the ability of CD40×EpCAM to promote uptake and cross-presentation of neoantigen contained in tumor-derived debris or exosomes, resulting in an increased priming of neoantigen-specific T cells.

CD40×EpCAM bsAb treatment induces TAA-dependent antitumor effect superior to monotargeting compounds

The antitumor effects of CD40×EpCAM and the mono-targeting CD40 mAb were compared in hCD40tg mice with established MB49-EpCAM tumors (figure 3A), which is an inflamed tumor model (online supplemental figure S2). Treatment with CD40×EpCAM bsAb at day 10, 13 and 16 (167 µg/dose) lead to a significantly reduced tumor volume (figure 3B) and increased survival (figure 3C) in mice bearing MB49 tumors with an established but heterogenous expression of EpCAM (figure 3D). In contrast, treatment with equivalent molar amounts of CD40 mAb (100 µg/dose) or isotype×EpCAM (167 µg/dose), administered separately or in combination, did not induce significant effects on tumor volume or survival compared with vehicle in this setting. Superior antitumor efficacy of CD40×EpCAM compared with CD40 mAb has been demonstrated in multiple experiments (data not shown). In this model system, the maximal effective dose was estimated to be between 167 µg and 417 µg (online supplemental figure S3).

To confirm that the antitumor activity of CD40×EpCAM observed in vivo was EpCAM-dependent, the effect of CD40×EpCAM was compared in hCD40tg mice bearing
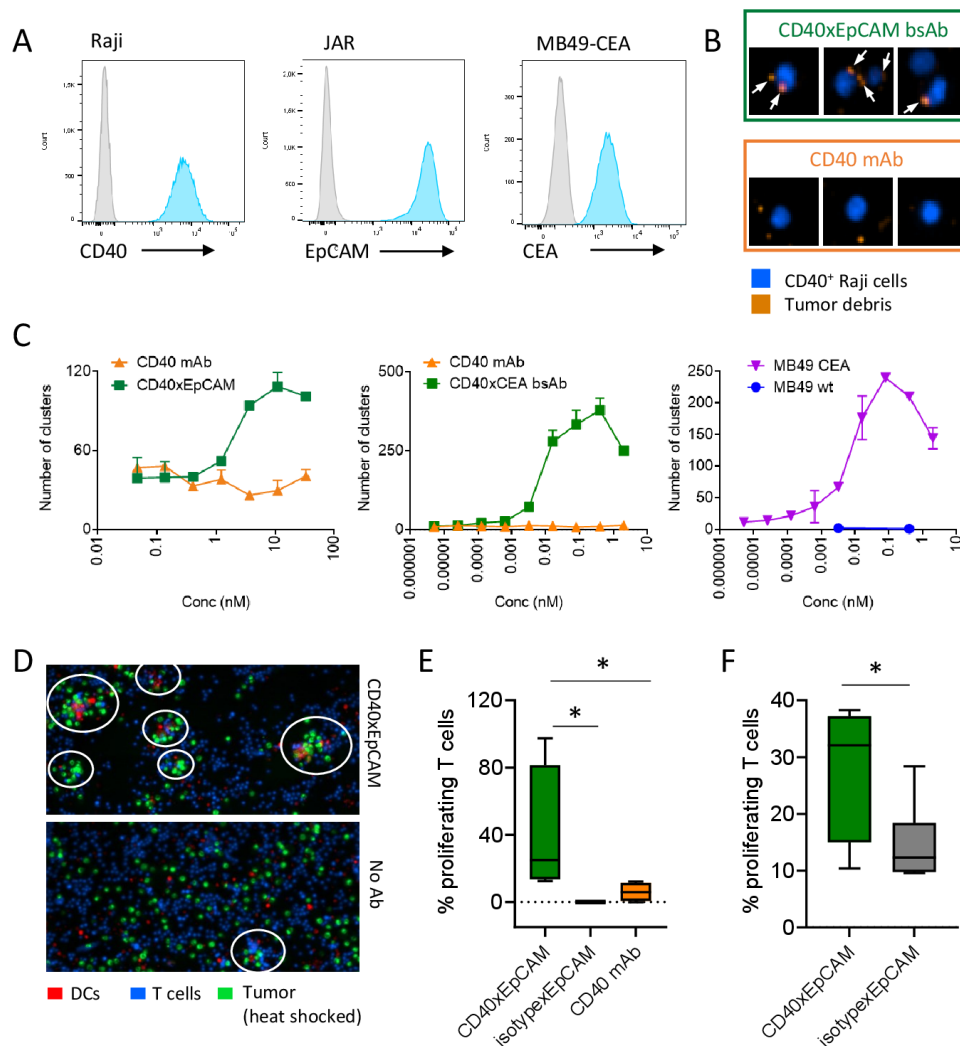
Figure 2 CD40×TAA bsAbs mediate localization of tumor debris to antigen presenting cells and promotes expansion of tumor antigen-specific T cells. (A) CD40 expression on Raji cells, EpCAM expression on JAR cells and CEA expression on MB49-CEA cells was verified using flow cytometry. Gray lines represent FMO controls, blue lines represent stained samples. (B) Fluorescently labeled CD40+ Raji cells were cultured with fluorescently labeled EpCAM+ tumor debris in the presence of titrated CD40 mAb or CD40×EpCAM bsAb. Images were captured using a live cell imaging system. (C) The number of EpCAM+ or CEA+ tumor debris clustering with CD40+ cells was quantified after 8 hours of culture with CD40 mAb, CD40×EpCAM or CD40×CEA using live cell imaging software. The graphs show the mean (+SD) of duplicate wells in one representative experiment of five (EpCAM), four (CEA) and eight for MB49-CEA+MB49 wt. (D) Fluorescently labeled DCs from CD40tg mice were cultured with fluorescently labeled heat-shocked MB49 tumor cells expressing human EpCAM and membrane bound ovalbumin (OVA) and CellTrace Violet-labeled TCR transgenic OVA-specific T cells (OT-1 T cells) in the presence or absence of CD40×EpCAM. Images were captured after 12 hours of co-culture. (E) The proliferation of OT-1 T cells in the co-cultures was assessed by flow cytometry after 3 days culture in the presence of CD40×EpCAM, isotype×EpCAM or CD40 mAb. The graph shows the median and min–max of pooled data from four experiments with the isotype×EpCAM control background subtracted. (F) Similar cultures were set up using exosomes isolated from MB49-EpCAM-OVA cells instead of necrotic debris, and proliferation of the OT-1 T cells was again assessed by flow cytometry after 3 days. The graph shows the median and min–max of pooled data from seven experiments. Statistical analysis was performed using a Mann-Whitney test, * p<0.05. bsAbs, bispecific antibodies; CEA, carcinoembryonic antigen; DC, dendritic cell; EpCAM, epithelial cell adhesion molecule.

MB49-EpCAM tumors or wildtype MB49 tumors without EpCAM expression (MB49-wt), respectively (figure 3E). In this experiment, the mice were i.p. treated with CD40×EpCAM (417 µg/dose) on day 10, 13, and 17. The results show that while treatment with CD40×EpCAM completely abrogated MB49-EpCAM tumor growth and led to survival of all mice in the MB49-EpCAM group, no mice in the MB49-wt tumor group survived (figure 3F,G),

indicating that the induction of the antitumor effects by CD40×EpCAM is dependent on EpCAM expression on the tumor cells.

In a different mouse model where s.c. injection of CEA-transfected MC38 cells was used to induce solid tumors in hCD40tg mice, treatment with a CD40×CEA bsAb (167 µg/dose) demonstrated similar antitumor effects as seen for CD40×EpCAM in the hCD40tg/MB49-EpCAM
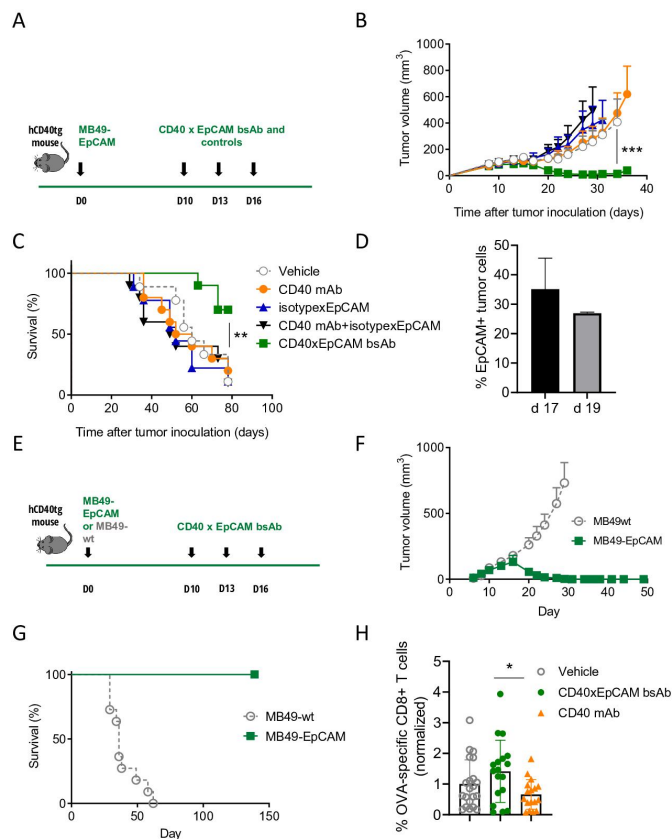
Figure 3 CD40×EpCAM treatment induces an EpCAM-dependent antitumor effect superior to CD40 and EpCAM monotargeting compounds alone or in combination. (A–C) MB49-EpCAM tumor-bearing hCD40tg mice were i.p. treated with vehicle control (PBS), 100 µg CD40 mAb, 167 µg isotype×EpCAM bsAb, 100 µg CD40 mAb plus 167 µg isotype×EpCAM bsAb, or 167 µg CD40×EpCAM on day 10, 13 and 16. (D) Percentage of EpCAM positive tumor cells in tumors analyzed at day 17 and day 19 using flow cytometry. (E–G) hCD40tg mice bearing either MB49-wt or MB49-EpCAM were i.p. treated with 417 µg CD40×EpCAM on day 10, 13 and 17. Tumor volume (B,F) and survival (C, G) were monitored. The graphs show the mean (+SEM) of 9–10 mice per group in one experiment (B, C) or of 11 mice per group in one representative experiment of three (F, G). (H) OT-1 T cells were adoptively transferred to hCD40tg mice bearing MB49-EpCAM-OVA tumors, followed by i.p. administration of 167 µg CD40×EpCAM or 100 µg CD40 mAb. Mice were subsequently treated with FTY720 to prevent T cell egress from lymph nodes, and the frequency of OVA-specific CD8$^+$ T cells in tumor draining lymph nodes was assessed 3 days after antibody administration. The graph shows the mean +/- SD of normalized and pooled data from three experiments. Statistical analysis of tumor volume and OVA-specific T-cell frequency was performed using a Mann-Whitney test, and survival using Kaplan-Meier log-rank. *p<0.05; ** p<0.01; *** p<0.001. bsAbs, bispecific antibodies; CEA, carcinoembryonic antigen; EpCAM, epithelial cell adhesion molecule; i.p., intraperitoneal; OVA, ovalbumin; s.c., subcutaneous.

model (online supplemental figure S4), indicating that the mechanism of action of the Neo-X-Prime bsAbs is valid for multiple appropriately expressed TAAs.

To investigate Neo-X-Prime bsAb-mediated priming of T cells in vivo, OT-1 T cells were adoptively transferred to hCD40tg mice bearing MB49-EpCAM-OVA tumors. The mice were treated with CD40×EpCAM bsAb, CD40 mAb or vehicle followed by FTY720 treatment to prevent T-cell egress from lymph nodes and allow inclusion of all cells primed in the tumor-draining lymph nodes in the analysis. Three days after antibody treatment, expansion of OT-1 T cells was seen in all treatment groups, with a tendency of a more efficient expansion of OT-1 T cells in mice treated with CD40×EpCAM bsAb compared with CD40 mAb (figure 3H). A similar trend was seen in three separate experiments (online supplemental figure S6). Further, treatment of male hCD40tg mice bearing MB49-EpCAM-OVA tumors with CD40×EpCAM bsAb but not CD40 mAb led to reduced tumor growth and increased survival (online supplemental figure S7) supporting the concept in an additional in vivo model.

Neo-X-Prime CD40×EpCAM bsAbs induce MB49 tumor-specific immunological memory

Next, we wanted to investigate whether treatment with CD40×EpCAM bsAb led to development of immunological memory towards MB49 tumor antigens. Thus, naïve mice and mice that had previously been cured from MB49-EpCAM tumors by CD40×EpCAM bsAb treatment (CR mice) were inoculated with MB49-EpCAM and MB49-wt tumor cells, respectively, in opposite flanks (figure 4A). MB49-EpCAM tumors grew in naïve but not CR mice, indicating that CR mice had developed immunological memory towards MB49-EpCAM in response to CD40×EpCAM treatment (figure 4B). Similarly, MB49-wt tumors grew in naïve but not CR mice, indicating that the immunological memory response was directed against antigens beyond EpCAM present in MB49 tumors (figure 4C).

The existence of EpCAM-independent MB49-specific immunological memory was further demonstrated by inoculating naïve or CR mice with MB49-wt cells or cells from an irrelevant tumor cell line (B16.F10) in opposite flanks. While MB49-wt tumors grew only in naïve mice, B16.F10 grew in both naïve and CR mice at comparable rates (figure 4D,E), indicating that CR mice had acquired MB49-wt-specific immunological memory and consequently protection against MB49 tumor growth as a result of CD40×EpCAM treatment.

To investigate whether the CD40×EpCAM-induced immunological memory response was driven by T cells, CR or naïve control mice were treated with T-cell-depleting antibodies or vehicle control on day -2, -1, 0, 4, 8, 11 and 15 with inoculation of MB49-EpCAM tumor cells on day 0. Tumor growth was observed in CRs treated with T-cell depleting antibodies but not vehicle control, indicating that the immunity to MB49 tumors in CR mice was dependent on T cells (figure 5).

Neo-X-Prime CD40×TAA bsAb treatment is not associated with systemic inflammation

To assess whether the antitumor immune response induced by CD40×EpCAM bsAb treatment was associated
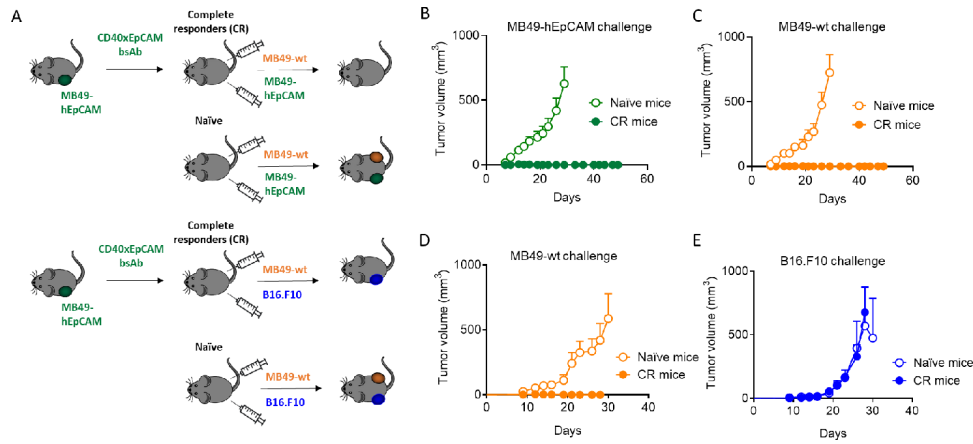
Figure 4 Mice cured from MB49-EpCAM tumors by CD40×EpCAM treatment develop MB49 tumor-specific immunological memory. (A) Naïve CD40tg mice or complete responders (CR) cured from MB49-EpCAM$^+$ tumors by CD40×EpCAM treatment were rechallenged with the same tumor on one flank and a MB49-wt tumor on the other flank. Alternatively, naïve or CR mice were rechallenged with MB49-wt or an irrelevant tumor (B16.F10) on opposite flanks. (B) Growth of MB49-EpCAM tumors and (C) MB49-wt tumors in CR and naïve mice was monitored. Following rechallenge with MB49-wt tumor on one flank and B16.F10 on the other flank, growth of (D) MB49-wt and (E) B16.F10 tumors in CR and naïve mice was monitored. Graphs show the mean (+SEM) of (B–C) 10 naïve and 19 CR mice in one representative experiment of three, or (D–E) 7 naïve and 11 CR mice in one experiment. EpCAM, epithelial cell adhesion molecule.

with systemic immune activation, hCD40tg mice were inoculated with MB49-EpCAM tumor cells and treated on day 10, 13 and 16 with CD40×EpCAM bsAb or CD40 mAb (wt IgG1). A CD40 superagonistic mAb known to
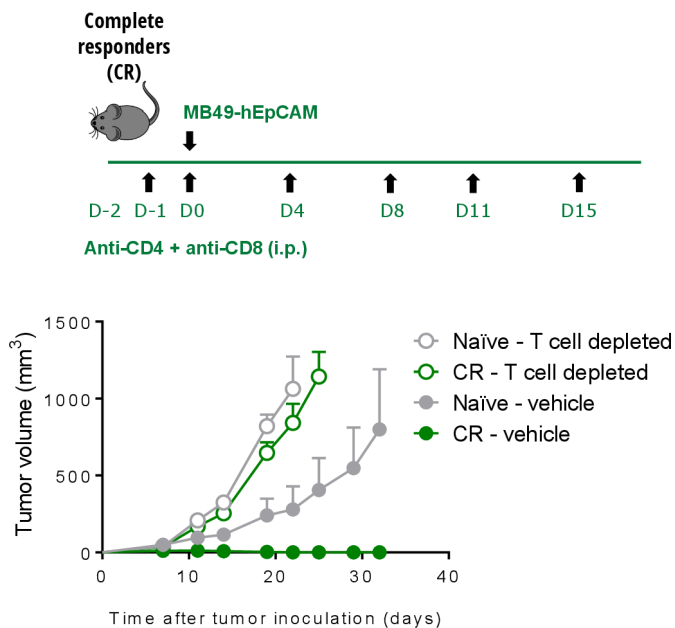
Figure 5 Immunological memory to MB49 tumors is dependent on T cells. Naïve C57bl/6 mice or hCD40tg CR mice cured from MB49-EpCAM$^+$ tumors by CD40×EpCAM treatment were treated with a combination of antibodies targeting CD4 and CD8 intending to deplete T cells, or with vehicle control (PBS) on days −2, −1, 0, 4, 8, 11 and 15. MB49-EpCAM tumor cells were inoculated s.c. on day 0 and tumor growth was monitored. The graph shows the mean (+SEM) of 10 CR and 3–4 naïve mice per group. CR, complete responders; EpCAM, epithelial cell adhesion molecule; PBS, phosphate-buffered saline; s.c., subcutaneous.

induce CD40-driven systemic immune activation was also included as a positive control. Analysis of secreted analytes in blood plasma, collected 4 hours after treatment administration on day 13, showed a significant increase in IL-6 levels in mice treated with CD40 mAb, in particular with the superagonistic control, but not after treatment with CD40×EpCAM bsAb, compared with vehicle control (figure 6A). The IL-6 levels also correlated well with the spleen weight, which was increased following treatment with the monospecific CD40 antibodies but not in mice treated with CD40×EpCAM bsAb (figure 6B). The same cytokine pattern was observed for a range of cytokines detected with a 19-plex assay (figure 6C). One exception was IL-15, where treatment with the higher dose of CD40×EpCAM seemed to promote elevated plasma levels to a similar or higher extent than the CD40 mAb. IL-33 appeared to follow a similar pattern although the levels detected were very low (figure 6C). In addition, a pilot toxicology study in non-human primates demonstrated that a Neo-X-Prime bsAb (CD40×CEA) was well tolerated up to 37.5 mg/kg, with no adverse findings or treatment-related changes in cytokine levels or liver enzymes (online supplemental figure S8). Taken together, these data suggest that CD40×TAA can be administered at effective dose levels without inducing systemic immune activation in this setting.

DISCUSSION

Herein, we describe conditionally active bsAbs targeting CD40 and highly expressed TAA such as EpCAM and CEA, designed to enhance cross priming of tumor-specific CD8$^+$ T cells, an approach we have named Neo-X-Prime. Using in vitro assays, we confirmed that the CD40×CEA and CD40×EpCAM bsAbs mediate TAA-conditional activation
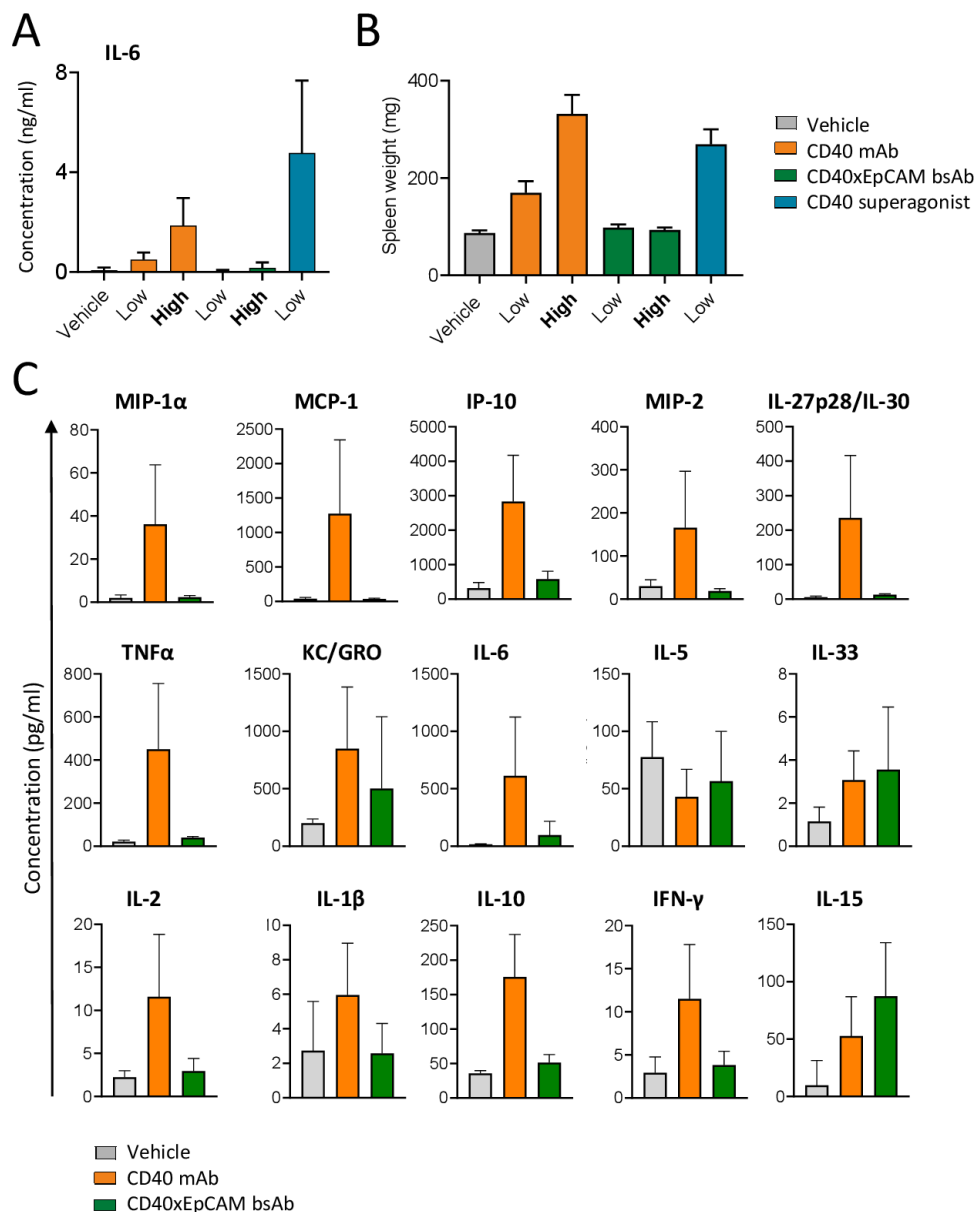
Figure 6 CD40×EpCAM treatment is not associated with elevated systemic cytokine levels. hCD40tg mice were inoculated with MB49-EpCAM$^+$ cells s.c. and administered 100 (low) or 250 µg (high) CD40 mAb, or molar equivalent doses (167 or 417 µg) CD40×EpCAM bsAb, or 100 µg of a CD40 superagonist i.p. on days 10, 13 and 16. Blood was collected 4 hours after antibody treatment on day 13, and (A) IL-6 levels in plasma were assessed by ELISA. (B) Spleen weight at sacrifice on day 20. (C) Remaining plasma samples were analyzed using a 19-plex mouse cytokine MSD panel. Results of analytes above lower limit of detection from mice treated with vehicle control or molar equivalent high doses of CD40 mAb or CD40×EpCAM bsAb are shown. The graphs show the mean (+SD) of (A) 5–6, (B) 6, or (C) 4–6 mice per group in one experiment. bsAbs, bispecific antibodies; EpCAM, epithelial cell adhesion molecule; IL, interleukin; i.p., intraperitoneal mAb, monoclonal antibody; s.c., subcutaneous.

of human APCs such as B cells and MoDCs. This study is the first to describe that the enhanced cross-priming obtained with CD40×TAA bsAbs translates into antitumor effect in vivo that is superior to CD40 mono-targeting compounds, without inducing signs of systemic immune activation. Further, similar results were obtained using a CD40×CEA bsAb in a colon cancer model (MC38-CEA), strongly supporting that the superior antitumor effects achieved with Neo-X-Prime antibodies, exemplified by both CD40×EpCAM and CD40×CEA, is not limited to a

specific tumor model and that the Neo-X-Prime concept can be applied across a variety of appropriately expressed TAA targets. Functional assays using a limited set of primary human cancer samples confirmed that the CEA levels in patients with colorectal cancer are sufficient to mediate CD40 clustering and demonstrated that tumor infiltrating immune cells can be activated using Neo-X-Prime bsAbs.

Our hypothesis is that the increased antitumor effects of Neo-X-Prime bsAbs compared with the mAbs is

mediated at least in part by engaging tumor-derived material (tumor debris, tumor derived vesicles and exosomes) containing tumor neoantigens with myeloid cells such as DCs. This is achieved by concomitant binding to TAAs on the tumor-derived material and CD40 expressed on the DCs, resulting in improved DC-mediated cross-priming of tumor-specific CD8^{+} T cells, which may increase the clonality of the tumor-specific T-cell response. While we cannot discern between cross-presentation and transfer of MHC/peptide complex via the tumor-derived material, both mechanisms result in the intended cross-priming of tumor-specific T cells. Indeed, our results show that both CD40×CEA and CD40×EpCAM bsAbs but not a CD40 mAb mediated clustering of tumor cell line-derived debris with CD40^{+} APCs in vitro, and that CD40xEpCAM treatment appeared to promote a more efficient expansion of tumor neoantigen-specific T cells in tumor-draining lymph nodes compared with CD40 mAb in vivo. Further, CD40×EpCAM bsAb improved DC uptake and cross-priming of tumor neoantigen-specific T cells in response to tumor debris or exosomes. Our hypothesis is further supported by in vitro data recently published by Sum *et al*, demonstrating that CD40×CEA antibodies can promote loading of DC with tumor antigen resulting in enhanced tumor-specific cross-priming.[24] In addition, the ability of CD40 to target tumor antigens for cross-presentation has been demonstrated previously using CD40 antibodies fused to tumor antigen peptides, resulting in efficient priming and activation of CD8^{+} T cells indicating that CD40 is superior to other DC targets in this regard.[11] Taken together, these data support the hypothesis that CD40-directed uptake of tumor material and priming of tumor antigen-specific CD8^{+} T cells contributes to the superior antitumor effect of CD40×EpCAM compared with CD40 mAb.

Other potential contributing factors to the increased antitumor efficacy could be that Neo-X-Prime antibodies activate CD40-expressing cells more strongly than CD40 mAbs in the TME supported by the fact that CD40×CEA bsAb localizes to the tumor to a greater extent than the CD40 mAb (online supplemental figure S5). This mechanism has been proposed by Sum *et al* studying a CD40×FAP bsAb, aiming to localize CD40 activation to the tumor stroma.[18] They demonstrated that a high dose was needed for tumor localization and antitumor activity in line with our results (online supplemental figure S2). However, the main data in the study by Sum *et al* was generated in a model with FAP-transfected tumor cells, essentially making FAP a highly expressed tumor cell-associated target and thus a model system supporting the Neo-X-Prime approach. Similar data on a CD40×FAP bispecific fusion protein was also recently presented by Rigamonti *et al*.[25] While our initial analyses of the major tumor-infiltrating immune cell populations have not revealed clear and consistent differences between treatment groups (data not shown), further studies including high resolution approaches such as single cell RNA sequencing may provide additional insight into the mechanisms behind the antitumor effects of Neo-X-Prime bsAbs.

Developing bsAbs based on the Neo-X-Prime approach, achieving binding to and internalization of tumor-derived material such as EV or exosomes likely requires high expression levels (receptor density) of the TAA. We found that CD40×TAA bsAbs could mediate clustering of CD40^{+} cells and debris from tumor cell lines with high TAA expression levels but not low TAA expression levels (online supplemental figure S9), which could have contributed to the limited clinical effect of CD40 bsAbs targeting tumor mesothelin, an antigen expressed at low density.[26] While potentially limiting the application of Neo-X-Prime to certain TAA, the apparent expression threshold would prevent DC activation outside the tumor, thereby limiting systemic immune activation and enhancing the tolerability profile of this new drug class.

In addition to the ability to cluster tumor debris with APCs, TAA receptor density influences the ability of Neo-X-Prime bsAbs to activate CD40-expressing cells, which is important both from a safety and efficacy perspective. The data herein supports that the levels of CEA on patient-derived tumor cells are in a relevant range, whereas the data suggests that very limited activity is expected in non-tumor tissue, which is expected to express <2000 CEA/cell.[27] Apart from the target density, the affinities of the binders affect the functional activity of Neo-X-Prime antibodies, for example, the CD40 affinity affects potency, whereas the CEA affinity, at least in some circumstances, does not (online supplemental figure S10).

The in vivo data confirm that CD40×EpCAM bsAb is a TAA-conditional agonist, as the presence of EpCAM on the tumor cells was necessary to induce antitumor effects. Furthermore, the treatment induced a T-cell memory response towards the wild type MB49 tumor and not a response restricted to the TAA (EpCAM). This suggests that Neo-X-Prime bsAbs induce cross-priming of T cells and the resulting antitumor activity is not limited to cancers that homogenously express high levels of tumor antigens, which is important as TAA expression in tumors often is heterogenous.[28] This contrasts Neo-X-Prime to CD3 bsAbs and ADCs, which are designed to kill TAA positive cells, but have a more limited capacity to induce a broad antitumor immunity.[28]

In conclusion, bispecific Neo-X-Prime antibodies targeting CD40 and TAA represent a promising novel treatment modality with the potential to meet key needs in immuno-oncology by expanding and activating tumor-specific T cells as well as potentially remodeling the TME to facilitate more efficient treatment of patients with cancer. CEA may be an ideal target for this purpose, based on the high expression level, relatively high tumor specificity and the data presented herein. We believe that the concept warrants clinical testing and are currently pursuing preclinical development of a Neo-X-Prime CD40×CEA bsAb.

ORCID iDs
David Gomez Jimenez http://orcid.org/0000-0002-9375-5263
Peter Ellmark http://orcid.org/0000-0002-6687-1250

REFERENCES

1 Sharma P, Hu-Lieskovan S, Wargo JA, *et al*. Primary, adaptive, and acquired resistance to cancer immunotherapy. *Cell* 2017;168:707–23.
2 Weiss SA, Sznol M. Resistance mechanisms to checkpoint inhibitors. *Curr Opin Immunol* 2021;69:47–55.
3 Beatty GL, Li Y, Long KB. Cancer immunotherapy: activating innate and adaptive immunity through CD40 agonists. *Expert Rev Anticancer Ther* 2017;17:175–86.
4 Vonderheide RH. CD40 agonist antibodies in cancer immunotherapy. *Annu Rev Med* 2020;71:47–58.
5 Hildner K, Edelson BT, Purtha WE, *et al*. Batf3 deficiency reveals a critical role for CD8alpha+ dendritic cells in cytotoxic T cell immunity. *Science* 2008;322:1097–100.
6 Sánchez-Paulete AR, Cueto FJ, Martínez-López M, *et al*. Cancer immunotherapy with immunomodulatory Anti-CD137 and anti-PD-1 monoclonal antibodies requires BATF3-Dependent dendritic cells. *Cancer Discov* 2016;6:71–9.
7 Caux C, Massacrier C, Vanbervliet B, *et al*. Activation of human dendritic cells through CD40 cross-linking. *J Exp Med* 1994;180:1263–72.
8 van Kooten C, Banchereau J. Immune regulation by CD40-CD40-L interactions. *Front Biosci* 1997;2:d1–11.
9 Gladue RP, Paradis T, Cole SH, *et al*. The CD40 agonist antibody CP-870,893 enhances dendritic cell and B-cell activity and promotes anti-tumor efficacy in SCID-hu mice. *Cancer Immunol Immunother* 2011;60:1009–17.
10 Bennett SR, Carbone FR, Karamalis F, *et al*. Help for cytotoxic-T-cell responses is mediated by CD40 signalling. *Nature* 1998;393:478–80.
11 Yin W, Gorvel L, Zurawski S, *et al*. Functional Specialty of CD40 and Dendritic Cell Surface Lectins for Exogenous Antigen Presentation to CD8(+) and CD4(+) T Cells. *EBioMedicine* 2016;5:46–58.
12 Mangsbo SM, Broos S, Fletcher E, *et al*. The human agonistic CD40 antibody ADC-1013 eradicates bladder tumors and generates T-cell-dependent tumor immunity. *Clin Cancer Res* 2015;21:1115–26.
13 Morrison AH, Diamond MS, Hay CA, *et al*. Sufficiency of CD40 activation and immune checkpoint blockade for T cell priming and tumor immunity. *Proc Natl Acad Sci U S A* 2020;117:8022–31.
14 Byrne KT, Vonderheide RH. CD40 stimulation obviates innate sensors and drives T cell immunity in cancer. *Cell Rep* 2016;15:2719–32.
15 van Mierlo GJD, den Boer AT, Medema JP, *et al*. CD40 stimulation leads to effective therapy of CD40(-) tumors through induction of strong systemic cytotoxic T lymphocyte immunity. *Proc Natl Acad Sci U S A* 2002;99:5561–6.
16 Enell Smith K, Deronic A, Hägerbrand K, *et al*. Rationale and clinical development of CD40 agonistic antibodies for cancer immunotherapy. *Expert Opin Biol Ther* 2021;21:1635–46.
17 Bajor DL, Mick R, Riese MJ, *et al*. Long-term outcomes of a phase I study of agonist CD40 antibody and CTLA-4 blockade in patients with metastatic melanoma. *Oncoimmunology* 2018;7:e1468956.
18 Sum E, Rapp M, Fröbel P, *et al*. Fibroblast activation protein α-Targeted CD40 agonism abrogates systemic toxicity and enables administration of high doses to induce effective antitumor immunity. *Clin Cancer Res* 2021;27:4036–53.
19 de Silva S, Fromm G, Shuptrine CW, *et al*. CD40 enhances type I interferon responses downstream of CD47 blockade, bridging innate and adaptive immunity. *Cancer Immunol Res* 2020;8:230–45.
20 Hagerbrand K, Levin M, Schantz LV, *et al*. 751 Neo-X-Prime bispecific antibodies targeting CD40 and tumor antigens promote cross-presentation of tumor exosome-derived neoantigen and induce superior anti-tumor responses compared to CD40 mAb. *Journal for ImmunoTherapy of Cancer* 2021;9:A785.
21 Yin W, Duluc D, Joo H, *et al*. Therapeutic HPV cancer vaccine targeted to CD40 elicits effective CD8+ T-cell immunity. *Cancer Immunol Res* 2016;4:823–34.
22 Flamar A-L, Xue Y, Zurawski SM, *et al*. Targeting concatenated HIV antigens to human CD40 expands a broad repertoire of multifunctional CD4+ and CD8+ T cells. *AIDS* 2013;27:2041–51.
23 Lund J, Pound JD, Jones PT, *et al*. Multiple binding sites on the CH2 domain of IgG for mouse Fc gamma R11. *Mol Immunol* 1992;29:53–9.
24 Sum E, Rapp M, Dürr H, *et al*. The tumor-targeted CD40 agonist CEA-CD40 promotes T cell priming via a dual mode of action by increasing antigen delivery to dendritic cells and enhancing their activation. *J Immunother Cancer* 2022;10:e003264.
25 Rigamonti N, Veitonmäki N, Domke C, *et al*. A multispecific anti-CD40 DARPin construct induces tumor-selective CD40 activation and tumor regression. *Cancer Immunol Res* 2022;10:626–40.
26 Ye S, Cohen D, Belmar NA, *et al*. A bispecific molecule targeting CD40 and tumor antigen mesothelin enhances tumor-specific immunity. *Cancer Immunol Res* 2019;7:1864–75.
27 Bacac M, Fauti T, Sam J, *et al*. A novel carcinoembryonic antigen T-cell bispecific antibody (CEA TCB) for the treatment of solid tumors. *Clin Cancer Res* 2016;22:3286–97.
28 Gonzalez-Exposito R, Semiannikova M, Griffiths B, *et al*. CEA expression heterogeneity and plasticity confer resistance to the CEA-targeting bispecific immunotherapy antibody cibisatamab (CEA-TCB) in patient-derived colorectal cancer organoids. *J Immunother Cancer* 2019;7:101.